

# Electronic excitations in anti-aromatic dehydro[12]- and aromatic dehydro[18]annulenes: a time-dependent density functional theory study

SMRITI ANAND<sup>†</sup> and H. BERNHARD SCHLEGEL<sup>\*‡</sup>

<sup>†</sup>Department of Chemistry and Institute for Scientific Computing, Wayne State University, Detroit, MI 48202, USA

<sup>‡</sup>Department of Biology, Chemistry and Environmental Science, Christopher Newport University, 1 University Place, Newport News, VA23606, USA

(Received 2 May 2005; in final form 15 June 2005)

The excited states of [12] and [18] dehydroannulenes have been studied using time-dependent density functional theory (TD-DFT). These compounds undergo intense intramolecular charge transfer between the terminal anilino groups and the central all-carbon core. The main geometric changes taking place on excitation are an increase in the C=C bond length and an increase in the adjacent C–C single bond. Protonation of the anilino groups causes only localized changes in the geometry but extensive changes in the excitation energies. The calculated transition energies and the shift in the absorption spectra upon protonation show a good qualitative agreement with the absorption spectra. The greater intensity of the absorption band in the aromatic [18]annulene can be attributed to contributions from two degenerate excited electronic states rather than aromatic/anti-aromatic effects.

## 1. Introduction

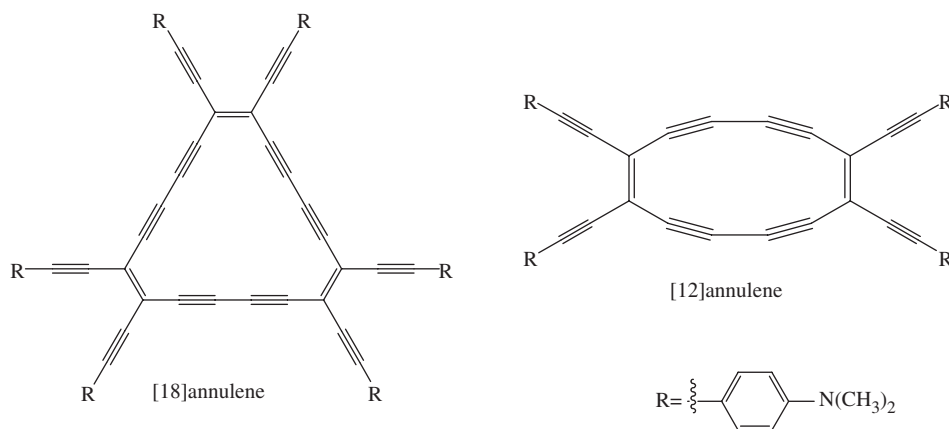
Dehydroannulenes and other acetylenic macrocycles have attracted a lot of interest in recent years because of their optoelectronic properties, aromaticity,  $\pi$  electron conjugation and use as precursors in the preparation of novel carbon containing compounds [1–22]. Even though the aromatic and anti-aromatic dehydroannulenes have been investigated for some time, very little is understood about the  $\pi$  electron conjugation across these macrocycles. Jusélius and Sundholm [12] investigated the structures and magnetic properties of some dehydro[12]- and [18]annulenes. Their studies show that the presence of fused benzene or cyclobutadiene rings destroys the aromaticity and anti-aromaticity of the dehydroannulenes while substitution of the ethynyl group has little or no effect. Nielsen and co-workers have prepared per(silylethynylated) dehydroannulenes and shown that the central all-carbon cores in these annulenes are strong electron acceptors [14]. A joint experimental and computational investigation has been carried out on N,N-dimethylaniline substituted tetraethynylethenes [23]. These systems

possess an emitting charge transfer (CT) state and the nature of the dual fluorescence was attributed to the twisted intramolecular charge transfer (TICT) model.

Recently, Mitzel *et al.* have synthesized N,N dimethyl-anilino substituted perethynylated dehydro[12]- and [18]annulenes [24, 25]. The [18]annulene is found to be aromatic in nature and the [12]annulene is anti-aromatic in nature. Both the systems are capable of mediating  $\pi$  electron donor–acceptor conjugation and undergo strong intramolecular charge transfer between the electron donating aniline groups and the electron accepting all-carbon core. Cyclic voltammetry (CV) studies on the [18]annulene confirmed the electron accepting property of the carbon core [24]. However, the intensity of the charge transfer (CT) band in [12]annulene is found to be weaker than that of [18]annulene [24]. This was contrary to expectations because the CT was expected to be efficient in the [12]annulene as it would enhance its aromaticity while the CT process would destroy the aromaticity of the [18]annulene.

The present study aims at understanding the nature of the excited states of these macrocycles in an effort to help elucidate the origin of the electronic transitions in these compounds. An explanation for the difference in the intensities of the CT bands in both the dehydroannulenes is provided. The systems studied were

\*Corresponding author. Email: hbs@chem.wayne.edu



Scheme 1.

N,N-dimethyl anilino substituted perethynylated octa-dehydro[12]annulene and dodecadehydro[18]annulene (see scheme 1).

## 2. Method

All the computational investigations were performed using the Gaussian suite of programs [26]. The ground state structures were optimized at the Hartree–Fock (HF) and B3LYP density functional theory [27, 28] and the excited states were studied using the configuration interaction (CIS) [29] and time-dependent density functional theory (TD-DFT) [30–32] methods with the STO-3G and 3-21G basis sets. The vertical excitation energies and oscillator strengths of the two annulenes were calculated. In a previous study of dodecadehydro-tribenzo[18]annulene [33], we found that the 3-21G basis set provided satisfactory agreement with the 6-31G(d) basis set calculation. It should be noted that larger basis sets and higher levels of theory would provide more accurate excitation energies and intensities.

## 3. Results and discussion

### 3.1. Structure

The ground state geometries of the systems shown in figure 1 are planar. The [12]annulene belongs to the  $D_{2h}$  point group while the [18]annulene belongs to the  $D_{3h}$  point group. The C≡C bond lengths in these systems are in the range of 1.18–1.23 Å and the C–C single bonds adjacent to the triple bond are about 1.39–1.40 Å. The geometric parameters thus are not affected by the aromaticity/anti-aromaticity. The molecules are quite flexible as evidenced by the presence of low frequency vibrational modes in the ground state. The [12]annulene has 24 vibrational modes with

frequencies less than  $100\text{ cm}^{-1}$  and the [18]annulene has 30. This may lead to the homogeneous broadening of the spectrum due to the motion of the perethynylated arms. The protonated forms of the annulenes were found to be planar as well. As seen from figure 1, protonation of the anilino groups does not cause any major geometric changes in the central all-carbon core, though the C–N bond lengths show an increase. Protonation also does not change the flexibility of the molecule. Thus, the acidification of the anilino groups in the annulenes may be regarded as a localized effect.

For the [12]annulene, the first two excited states with significant calculated oscillator strengths were optimized using the CIS method (see table 1 for the nomenclature and description of the excited states). The molecule retains its planarity in the excited state and the C≡C bond length increases by about 0.02 Å. In  $S_1$  the C≡C bond lengths in the side chains lengthen while in  $S_2$ , the C≡C in the ring lengthens reflecting the nature of the excited states. Since protonation does not affect the ground state geometry in these systems, one expects that the excited state geometries will also not be affected much by the protonation. Due to its large size, it was not practical to optimize the excited states of [18]annulene and only the excited state energies and oscillator strengths are discussed.

### 3.2. Molecular orbitals and excited states of the annulenes

The calculated excitation energies and oscillator strengths for the unprotonated and protonated forms of the annulenes are collected in table 1. The results show a qualitative agreement with the experimental absorption spectrum (figure 2). One must keep in mind that the CIS method tends to overestimate the excitation energies while the TD-DFT method underestimates the energy for charge transfer states [34–41]. The CIS

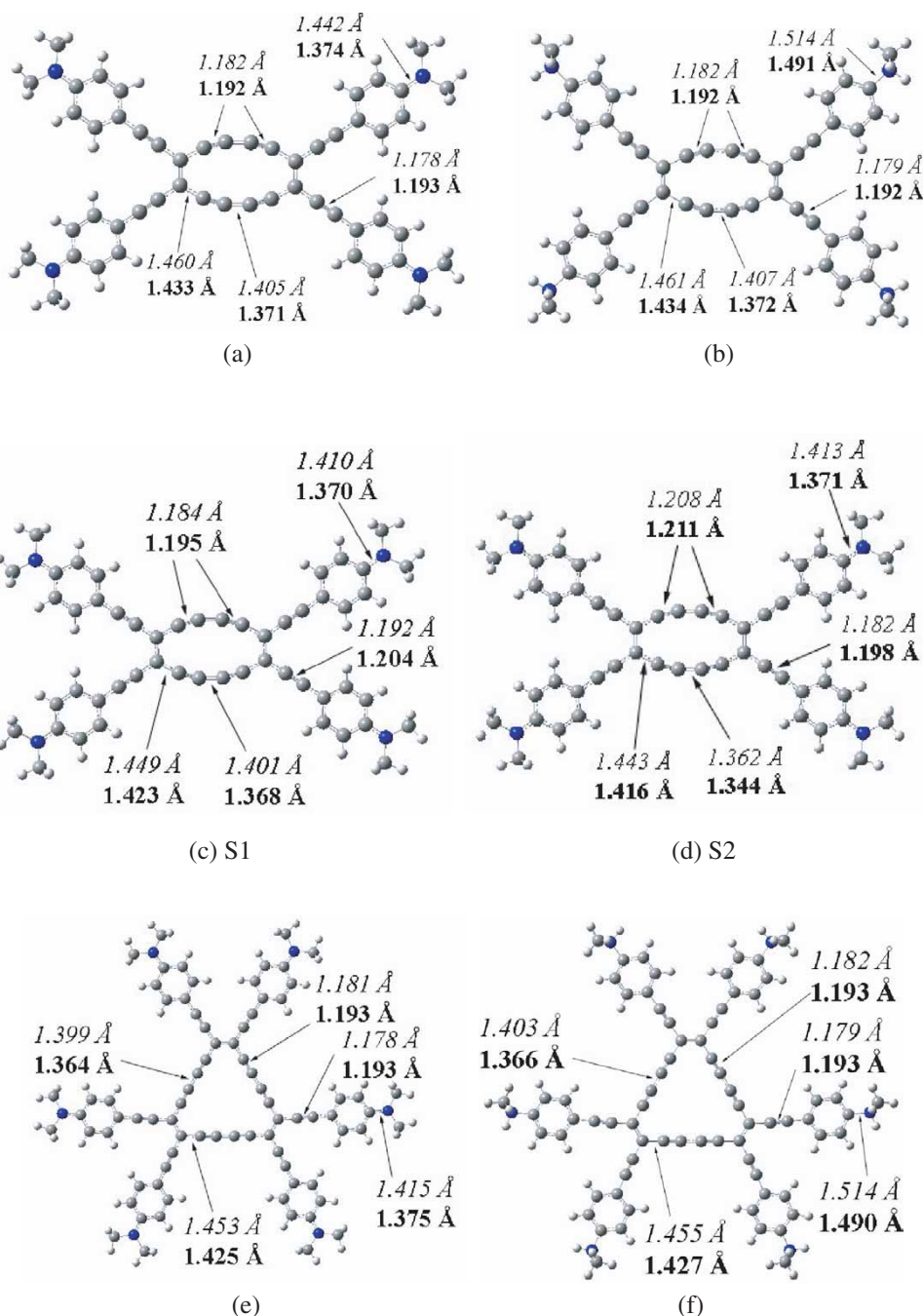


Figure 1. The structures of (a) ground state of [12]annulene, (b) ground state of protonated [12]annulene, (c) first and (d) second excited states of [12]annulene (at CIS), (e) ground state of [18]annulene and (f) ground state of protonated [18]annulene. Numbers in italics correspond to the STO-3G data and those in bold correspond to the 3-21G data.

method is also found to overestimate the oscillator strength by about 20% while the TD-DFT values are about 30% lower than the experimental value even in a small system like benzene [42]. Despite these limitations, CIS and TDDFT are sufficient to reproduce the qualitative trends for unprotonated versus protonated annulenes. Similar to our earlier results [33],

we find that the STO-3G basis set is sufficient for reproducing the trends but the 3-21G basis set shows a better agreement with the experimental data.

In the unprotonated [12]annulene, the TD-B3LYP/3-21G calculations show the presence of three states at 1.90, 2.28 and 2.68 eV with oscillator strengths ( $f$ ) of 0.305, 1.376 and 0.977, respectively. This qualitatively

Table 1. Excitation energies ( $\Delta E$  in eV) and oscillator strengths ( $f$ ) for the [12]- and [18]annulenes.

State (Transition description)	CIS/ STO-3G		CIS/ 3-21G		TD-B3LYP/ STO-3G		TD-B3LYP/ 3-21G		Experiment [24]	
	$\Delta E$	$f$	$\Delta E$	$f$	$\Delta E$	$f$	$\Delta E$	$f$	$\Delta E$	$\epsilon/\text{M}^{-1}\text{cm}^{-1}$
[12]annulene										
S1 (HOMO-1 $\rightarrow$ LUMO)	5.36	2.474	4.04	2.154	2.24	0.351	1.90	0.305	2.19	20000
S2 (HOMO-2 $\rightarrow$ LUMO)	6.04	2.398	4.68	2.684	2.57	1.195	2.28	1.376	2.39	35100
S3 (HOMO $\rightarrow$ LUMO+1)	6.67	1.207	5.47	1.218	3.08	0.956	2.68	0.977	2.91	22500
Protonated [12]annulene										
S1 (HOMO $\rightarrow$ LUMO+1)	7.18	0.008	5.76	0.006	2.66	0.062	2.33	0.013	2.17	–
S1 (HOMO-2 $\rightarrow$ LUMO)	5.59	2.736	4.39	2.562	3.28	1.554	2.85	1.602	3.26	34000
S2 (HOMO $\rightarrow$ LUMO+2)	6.09	1.097	4.84	1.234	3.51	1.994	3.21	1.701	3.87	35000
[18]annulene										
HOMO $\rightarrow$ LUMO ( $A_1'$ )	6.82	0.000	5.03	0.000	2.07	0.000	1.69	0.000	–	–
HOMO $\rightarrow$ LUMO ( $A_2'$ )	4.67	0.000	3.31	0.000	2.26	0.000	1.88	0.000	–	–
HOMO $\rightarrow$ LUMO ( $E'$ )	5.28	6.560	3.97	6.456	2.40	2.686	2.10	3.528	2.39	105200
Protonated [18]annulene										
HOMO $\rightarrow$ LUMO ( $A_1'$ )	6.98	0.000	5.12	0.000	2.23	0.000	1.84	0.000	–	–
HOMO $\rightarrow$ LUMO ( $A_2'$ )	4.70	0.000	3.39	0.000	2.41	0.000	2.02	0.000	–	–
HOMO $\rightarrow$ LUMO ( $E'$ )	5.42	6.188	4.17	6.108	2.75	3.842	2.41	4.163	2.90	98000

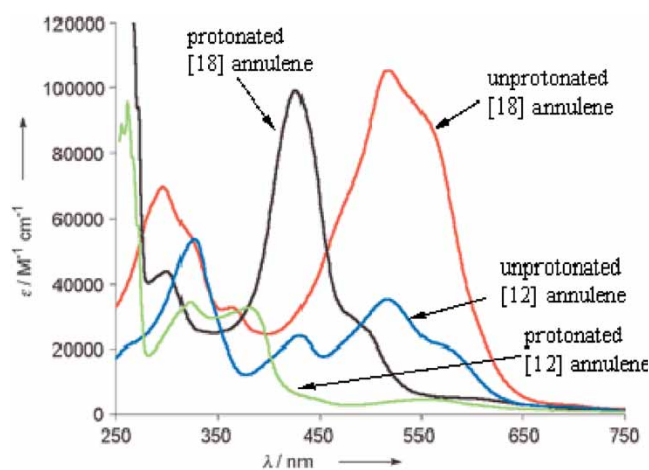


Figure 2. The spectrum of [12]annulene and [18]annulene. (From [24], reproduced by permission of The Royal Society of Chemistry.)

agrees with the experimental spectrum (in  $\text{CHCl}_3$ ) which shows bands at  $\sim 2.17$  ( $\sim 570$  nm),  $2.39$  (518 nm) and  $2.89$  eV (430 nm). When the anilino groups are protonated (by acidification with toluene-4-sulphonic acid), the most intense band at 518 nm disappears nearly completely and is replaced by two bands at approximately 385 and 325 nm. Neutralization of the solution (with triethyl amine) regenerates the original absorption spectrum and hence the band at 518 nm (calculated at 2.28 eV) was identified as a CT band [24].

TD-B3LYP/3-21G calculations on the protonated [12]annulene reproduce this trend with the intense transitions now appearing at 2.85 ( $f=1.60$ ) and 3.21 eV ( $f=1.70$ ). The calculated shift of 108 nm for the CT band is in qualitative agreement with the experimental shift of  $\sim 130$  nm. The spectrum of the protonated [12]annulene has a broad, low intensity band at 570 nm. The calculations show a very weak transition at 2.33 eV ( $f=0.013$ ), but it is more likely that the 570 nm band is due to incomplete protonation. The absorption spectrum of [18]annulene shows a strong band at 518 nm. Upon the protonation of the anilino groups, this band is replaced by a band at 427 nm. The shoulder at  $\sim 500$  nm in the spectrum was attributed to incomplete hexa-protonation [24]. In the protonated form, the lowest energy transition with significant oscillator strength is calculated to be at 2.41 eV compared to 2.10 eV in the unprotonated form (TD-B3LYP/3-21G data from table 1). The shift of 75 nm (TD-B3LYP/3-21G data) in the energy agrees qualitatively with the shift of 90 nm observed in the experimental spectrum. Including solvation effects in the calculations and using larger basis sets would improve the agreement with the observed excitation energies.

The lowest excited state in both the annulenes can be described as a  $\pi \rightarrow \pi^*$  transition involving charge transfer from the anilino groups to the central carbon core. These systems also show a  $\pi' \rightarrow \pi'^*$  transition

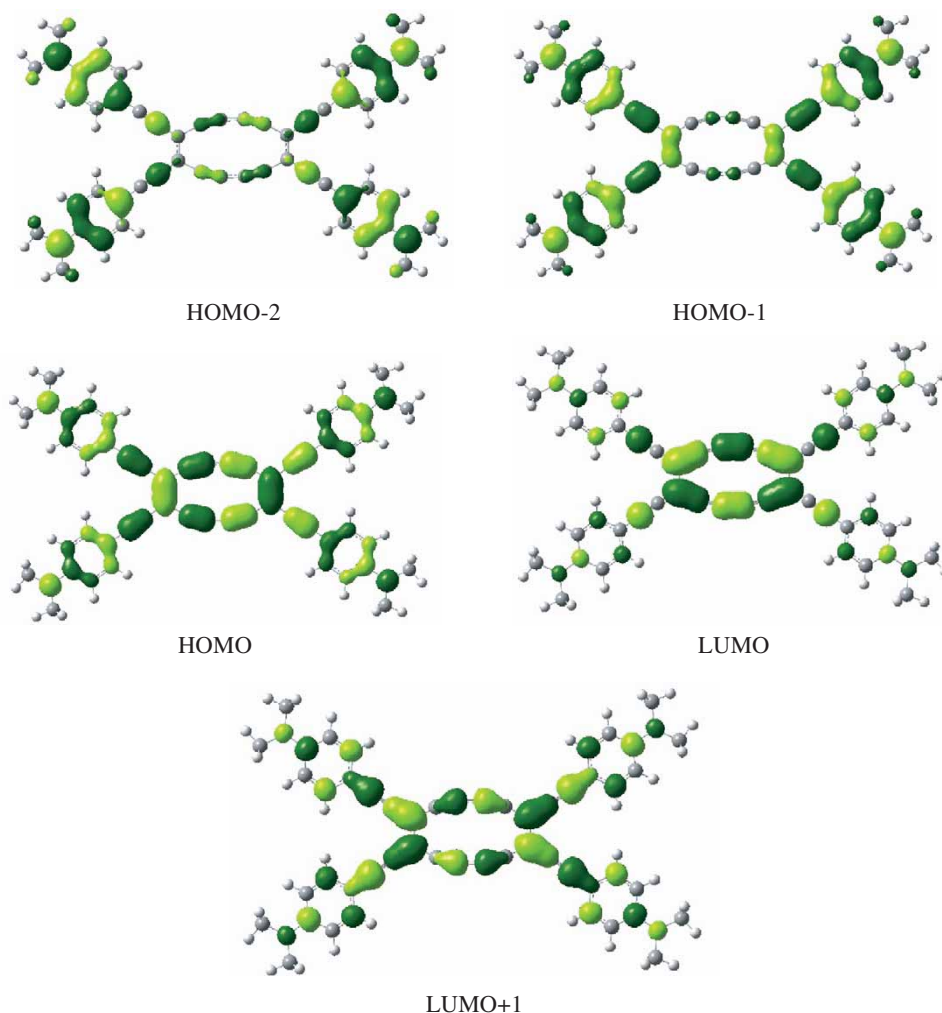


Figure 3. The molecular orbitals of [12]annulene.

involving the  $\pi$  orbitals of the  $C\equiv C$  that are in the plane of the molecule. These transitions are similar to systems studied earlier [33]. The molecular orbitals involved in the  $\pi \rightarrow \pi^*$  transitions are shown in figures 3 and 4. As seen from figure 3, the highest occupied molecular orbital (HOMO) of [12]annulene is delocalized over the carbon core and the anilino-ethynyl arms, and the conjugation between them is seen clearly. The lowest unoccupied molecular orbital (LUMO) is localized more on the central carbon core. On the other hand, the HOMO-1 and HOMO-2 orbitals are more localized on the anilino-ethynyl arms. Similarly, the HOMO-1 and HOMO-2 orbitals in the [18]annulene are also localized on the anilino-ethynyl arms (figure 4). It is clear from the figure that the HOMO (a pair of degenerate orbitals) is delocalized over the whole molecule and the LUMO (also degenerate) is localized more on the central carbon core.

The density difference between the ground state and the lowest three excited states with significant oscillator strength in the unprotonated [12]annulene is presented in figure 5 (see table 1 for description and nomenclature). The plots for the first two excited states clearly show the charge transfer between the anilino groups and the carbon core. The plot for the third excited state in figure 5 shows that the change in electron density is localized on the arms. In the protonated [12]annulene, the plot shows the transfer of the density from the core to the arms (see  $S_2$  in figure 6). The density difference plot for the unprotonated [18]annulene is presented in figure 7(a) and shows the charge transfer from the anilino groups to the carbon core. Similar to the protonated [12]annulene, the density difference plot for the protonated [18]annulene (figure 7(b)) also shows the charge transfer from the carbon core to the perethynylated arms.

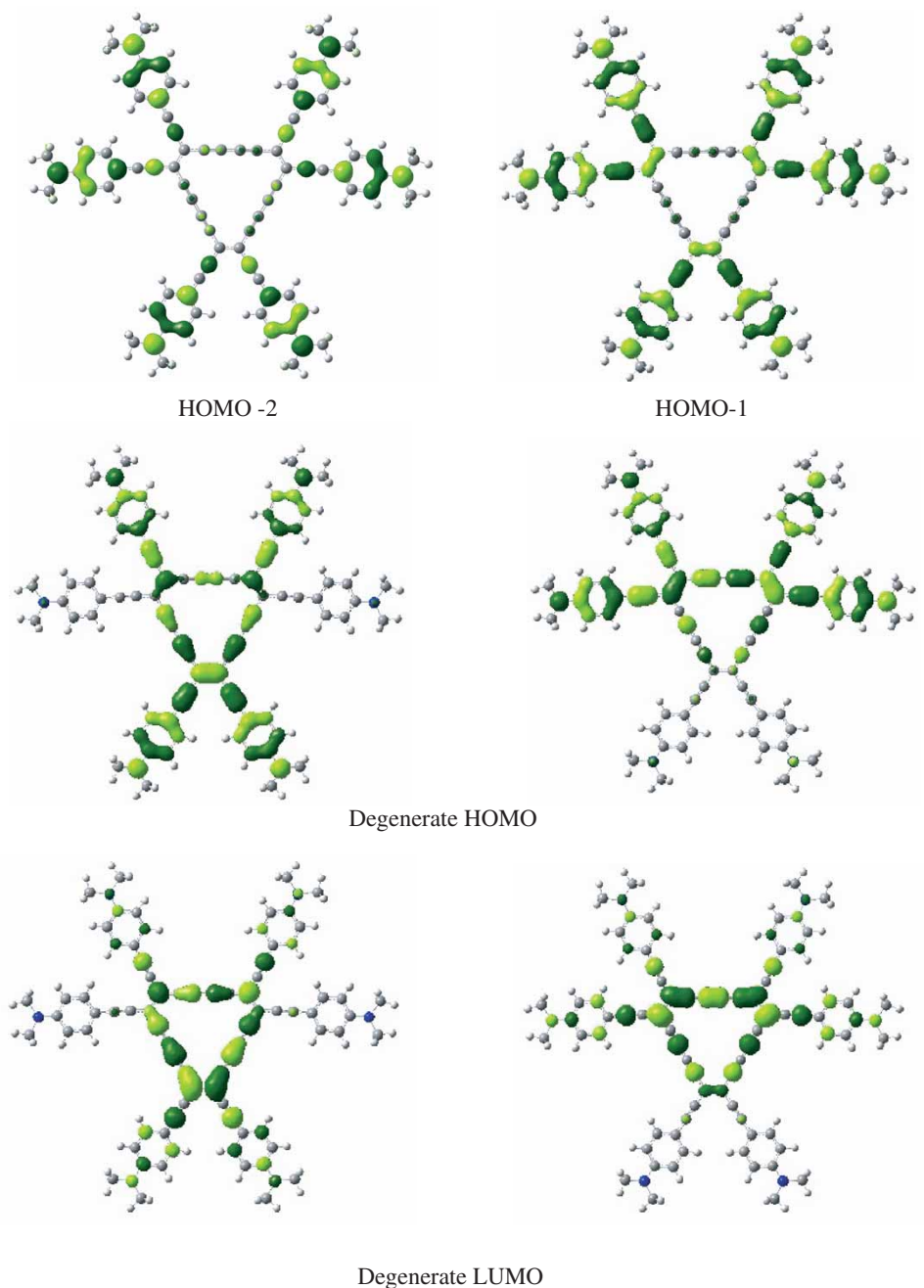


Figure 4. The molecular orbitals of [18]annulene.

### 3.3. The intensity of the CT bands

The intensity of the 518 nm CT band in [18]annulene is observed to be about three times that of the CT band in [12]annulene and this was found to be surprising [24]. The [12]annulene is anti-aromatic and CT is expected to be more efficient because the increase of the electron density in the carbon core would enhance its aromaticity. Since the [18]annulene is aromatic to begin with, CT should not be as efficient because its aromaticity

is destroyed due to the transfer of electron density into the carbon core.

To resolve this paradox and to understand the nature of the electronic excitation, the molecular orbitals of [18]annulene have to be examined in detail. As seen from figure 4, the HOMO is a pair of degenerate  $\pi$  orbitals of  $E''$  symmetry and so is the LUMO. A HOMO  $\rightarrow$  LUMO transition results in four states,  $E'' \times E'' = A'_1 + A'_2 + E'$ . The two  $A'$  states are dipole forbidden

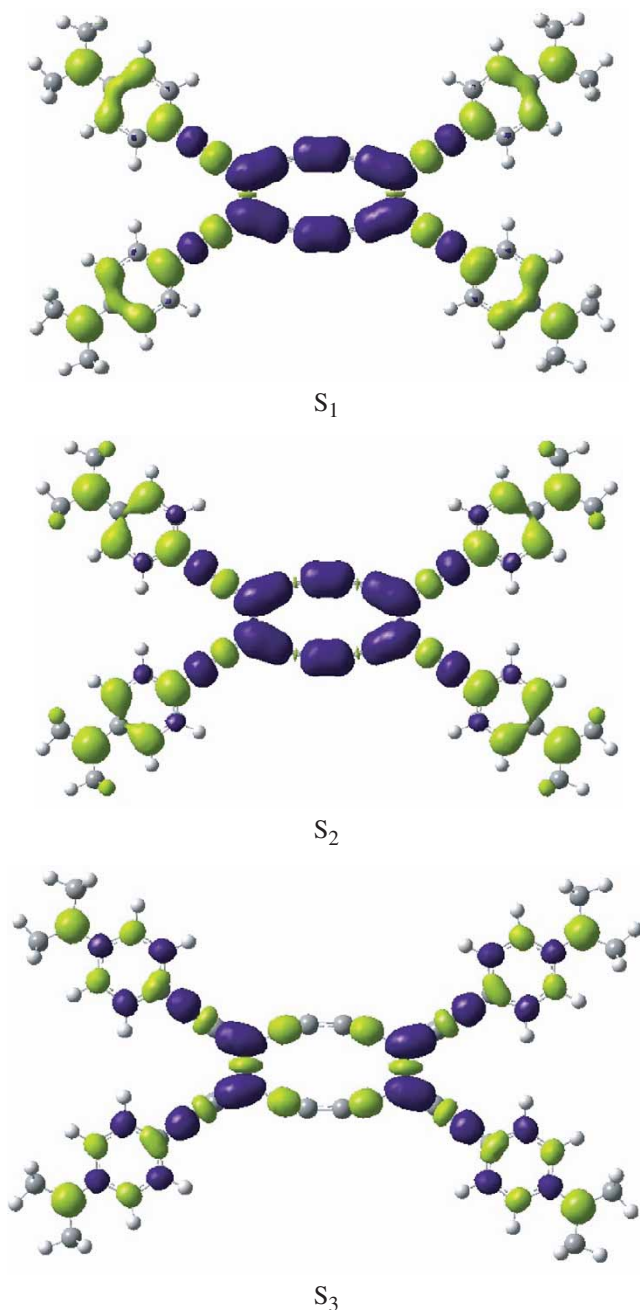


Figure 5. Density difference between the first three excited states at TD-B3LYP/STO-3G and the ground B3LYP/STO-3G state for unprotonated [12]annulene (see table 1 for description of the states). The darker, purple colour shows increased electron density in the excited state and the light green shows decreased electron density relative to the ground state. The movement of electron density from the arms to the core characterizes the charge transfer state.

by symmetry and hence have zero oscillator strength. The transition to the degenerate  $E'$  state is dipole allowed by symmetry. A similar situation occurs in benzene. TD-B3LYP calculations on [18]annulene

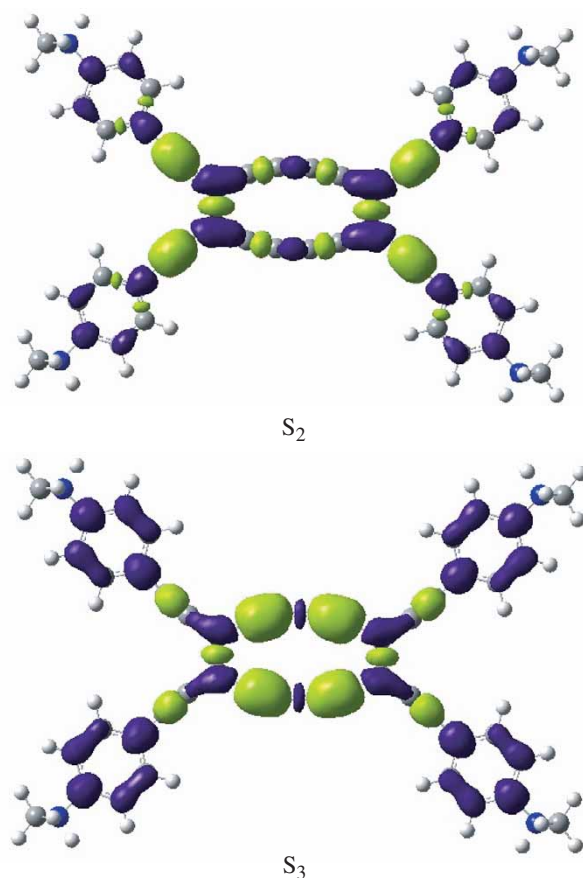


Figure 6. Density difference between the excited states at TD-B3LYP/STO-3G and the ground B3LYP/STO-3G state for protonated [12]annulene (see table 1 for description of the states). The darker, purple colour shows increased electron density in the excited state and the light green shows decreased electron density relative to the ground state. The movement of electron density from the arms to the core characterizes the charge transfer state.

show the presence of two  $A'$  states with zero oscillator strength which are lower in energy than the degenerate  $E'$  state which has significant oscillator strength. However, the CIS method places one of the  $A'$  states higher than the  $E'$  state (see table 1). A similar problem is found in the CIS calculation of the excited states of benzene [43] with the lowest  $B_{1u}$  transition being overestimated by about 2 eV. However, the TD-DFT calculation on [18]annulene places the  $A'$  states lower in energy than the degenerate  $E'$  state. Thus the most intense peak in the absorption spectrum of [18]annulene corresponds to a transition to the  $E'$  state. Since both the  $E'$  states contribute to the transition, the intensity of the peak is much greater in the [18]annulene. Figure 7(a) shows the density difference plot between the excited  $E'$  state and the ground state calculated at TD-B3LYP/STO-3G and is the sum of the plots for the two

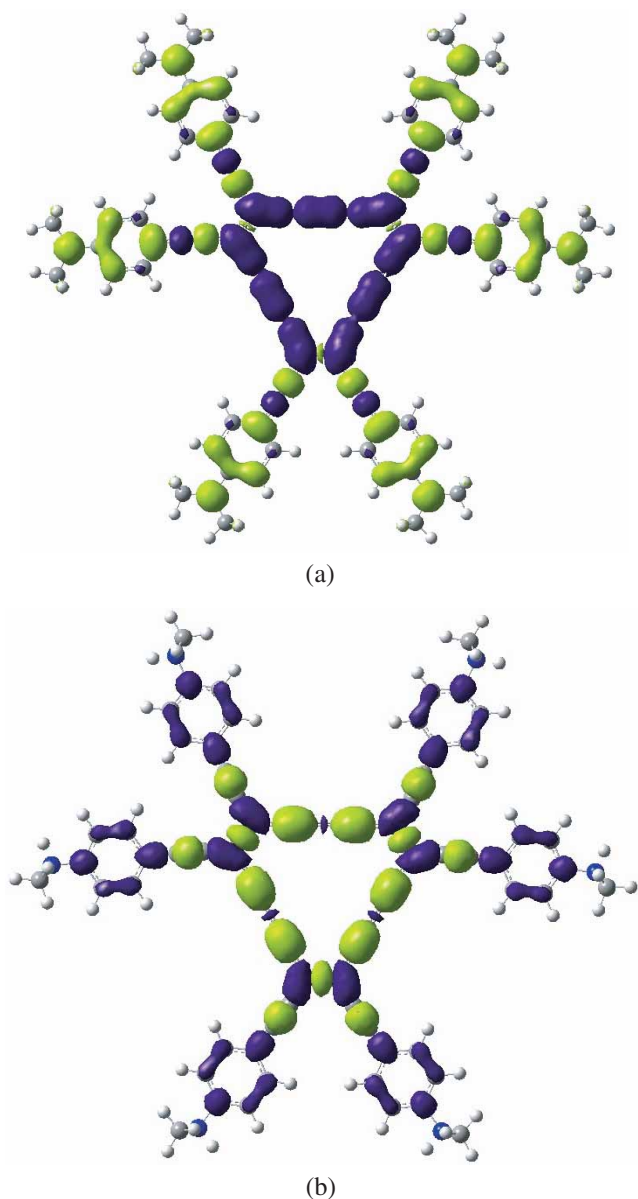


Figure 7. Sum of the density difference plots for the two  $E'$  excited states calculated at TD-B3LYP/STO-3G and the ground B3LYP/STO-3G state for (a) unprotonated and (b) protonated [18]annulene. The darker, purple colour shows increased electron density in the excited state and the light green shows decreased electron density relative to the ground state. The movement of electron density from the arms to the core characterizes the charge transfer state.

degenerate states. The oscillator strength for [18]annulene shown in table 1 is the sum of the oscillator strength of the two  $E'$  states. Although transitions to the  $A'$  states have zero intensity by symmetry at the equilibrium geometry, the molecule is very flexible and thermal motion could cause sufficient distortion for these transitions to pick up some intensity in both the neutral and the protonated [18]annulene.

Partial protonation of the anilino groups could also lower the symmetry so that these transitions could gain additional intensity, accounting for the pronounced shoulder observed in the spectrum of the protonated [18]annulene.

#### 4. Conclusion

The excited states of two dehydroannulenes have been studied using electronic structure theory calculations. The lowest excited states in both the [12]- and [18]annulene correspond to a  $\pi \rightarrow \pi^*$  transition involving intramolecular charge transfer between the anilino groups and the central all-carbon core. The calculated transition energies and oscillator strengths qualitatively reproduce the trends in the absorption spectra in both the unprotonated and the protonated annulenes. The transition in the aromatic dehydro[18]annulene is from the ground state to a degenerate excited state of  $E'$  symmetry. Thus, both the  $E'$  states contribute to the oscillator strength and this accounts for the greater intensity of the CT band in the absorption spectrum of the [18]annulene. The ratio of the calculated oscillator strength ([18]annulene: [12]annulene) is about 2.5 and agrees well with the ratio of 3 between the extinction coefficients.

#### Acknowledgements

This work was supported by grant from the National Science Foundation (CHE 051244). Computer time made available by C&IT and ISC is gratefully acknowledged.

#### References

- [1] F. Diederich, Y. Rubin, C. Knobler, R. L. Whetten, K. E. Schriver, and K. N. Houk, Y. Li, *Science* **245**, 1088 (1989).
- [2] Y. Li, Y. Rubin, F. Diederich, and K. N. Houk, *J. Am. Chem. Soc.* **112**, 1618 (1990).
- [3] F. Diederich, Y. Rubin, O. L. Chapman, and N. S. Goroff, *Helv. Chim. Acta* **77**, 1441 (1994).
- [4] J. Anthony, A. M. Boldi, C. Boudon, J. Gisselbrecht, M. Gross, P. Seiler, C. B. Knobler, and F. Diederich, *Chim. Acta Helv.* **78**, 797 (1995).
- [5] J. Anthony, A. M. Boldi, Y. Rubin, M. Hobi, V. Gramlich, C. B. Knobler, P. Seiler, and F. Diederich, *Helv. Chim. Acta* **78**, 13 (1995).
- [6] R. R. Tykwinski, M. Schreiber, R. Perez Carlon, F. Diederich, and V. Gramlich, *Helv. Chim. Acta* **79**, 2249 (1996).
- [7] R. R. Tykwinski, U. Gubler, R. E. Martin, F. Diederich, C. Bosshard, and P. Guenter, *J. Phys. Chem. B* **102**, 4451 (1998).

- [8] S. Eisler and R. R. Tykwinski, *Angew. Chem. Int. Ed.* **38**, 1940 (1999).
- [9] U. H. F. Bunz, Y. Rubin, and Y. Tobe, *Chem. Soc. Rev.* **28**, 107 (1999).
- [10] E. M. Garcia-Frutos, F. Fernandez-Lazaro, E. M. Maya, P. Vazquez, and T. Torres, *J. Org. Chem.* **65**, 6841 (2000).
- [11] M. J. Cook and M. J. Heeney, *Chem. Eur. J.* **6**, 3958 (2000).
- [12] J. Jusélius and D. Sundholm, *Phys. Chem. Chem. Phys.* **3**, 2433 (2001).
- [13] W. B. Wan and M. M. Haley, *J. Org. Chem.* **66**, 3893 (2001).
- [14] M. B. Nielsen, M. Schreiber, Y. G. Baek, P. Seiler, S. Lecomte, C. Boudon, R. R. Tykwinski, J.-P. Gisselbrecht, V. Gramlich, P. J. Skinner, C. Bosshard, P. Gunter, M. Gross, and F. Diederich, *Chem. Eur. J.* **7**, 3263 (2001).
- [15] M. Laskoski, M. D. Smith, J. G. M. Morton, and U. H. F. Bunz, *J. Org. Chem.* **66**, 5174 (2001).
- [16] G. J. Palmer, S. R. Parkin, and J. E. Anthony, *Angew. Chem. Int. Ed.* **40**, 2509 (2001).
- [17] T. Nishinaga, N. Nodera, Y. Miyata, and K. Komatsu, *J. Org. Chem.* **67**, 6091 (2002).
- [18] M. Laskoski, W. Steffen, J. G. M. Morton, M. D. Smith, and U. H. F. Bunz, *J. Am. Chem. Soc.* **124**, 13814 (2002).
- [19] T. Kawase, Y. Seirai, H. R. Darabi, M. Oda, Y. Sarakai, and K. Tashiro, *Angew. Chem. Int. Ed.* **42**, 1621 (2003).
- [20] C. Lepetit, M. B. Nielsen, F. Diederich, and R. Chauvin, *Chem. Eur. J.* **9**, 5056 (2003).
- [21] F. Mitzel, C. Boudon, J.-P. Gisselbrecht, P. Seiler, M. Gross, and F. Diederich, *Chem. Commun.* 1634 (2003).
- [22] J. A. Marsden, G. J. Palmer, and M. M. Haley, *Eur. J. Org. Chem.* 2355 (2003).
- [23] L. Gobbi, N. Elmaci, H. P. Luthi, and F. Deidrich, *Chem. Phys. Chem.* **2**, 423 (2001).
- [24] F. Mitzel, C. Boudon, J.-P. Gisselbrecht, M. Gross, and F. Diederich, *Chem. Commun.* 2318 (2002).
- [25] F. Mitzel, C. Boudon, J.-P. Gisselbrecht, P. Seiler, M. Gross, and F. Diederich, *Helv. Chim. Acta* **87**, 1130 (2004).
- [26] M. J. Frisch, G. W. Trucks, H. B. Schlegel, G. E. Scuseria, M. A. Robb, J. R. Cheeseman, J. A. Montgomery Jr, T. Vreven, K. N. Kudin, J. C. Burant, J. M. Millam, S. S. Iyengar, J. Tomasi, V. Barone, B. Mennucci, M. Cossi, G. Scalmani, N. Rega, G. A. Petersson, H. Nakatsuji, M. Hada, M. Ehara, K. Toyota, R. Fukuda, J. Hasegawa, M. Ishida, T. Nakajima, Y. Honda, O. Kitao, H. Nakai, M. Klene, X. Li, J. E. Knox, H. P. Hratchian, J. B. Cross, C. Adamo, J. Jaramillo, R. Gomperts, R. E. Stratmann, O. Yazyev, A. J. Austin, R. Cammi, C. Pomelli, J. W. Ochterski, P. Y. Ayala, K. Morokuma, G.A. Voth, P. Salvador, J. J. Dannenberg, V.G. Zakrzewski, S. Dapprich, A. D. Daniels, M. C. Strain, O. Farkas, D. K. Malick, A. D. Rabuck, K. Raghavachari, J. B. Foresman, J. V. Ortiz, Q. Cui, A. G. Baboul, S. Clifford, J. Cioslowski, B. B. Stefanov, G. Liu, A. Liashenko, P. Piskorz, I. Komaromi, R. L. Martin, D. J. Fox, T. Keith, M. A. Al-Laham, C. Y. Peng, A. Nanayakkara, M. Challacombe, P. M. W. Gill, B. Johnson, W. Chen, M. W. Wong, C. Gonzalez, and J. A. Pople, *Gaussian 03*, revision D.01 (development version) (Gaussian Inc., Wallingford CT, 2004).
- [27] A. D. Becke, *Phys. Rev. A* **38**, 3098 (1988).
- [28] A. D. Becke, *J. Chem. Phys.* **98**, 1372 (1993).
- [29] J. B. Foresman, M. Head-Gordon, J. A. Pople, and M. J. Frisch, *J. Phys. Chem.* **96**, 135 (1992).
- [30] R. Bauernschmitt and R. Ahlrichs, *Chem. Phys. Lett.* **256**, 454 (1996).
- [31] M. E. Casida, C. Jamorski, K. C. Casida, and D.R. Salahub, *J. Chem. Phys.* **108**, 4439 (1998).
- [32] R. E. Stratmann, G. E. Scuseria, and M. J. Frisch, *J. Chem. Phys.* **109**, 8218 (1998).
- [33] S. Anand, O. Varnavski, J. A. Marsden, M. M. Haley, H. B. Schlegel, and T. Goodson III, *J. Phys. Chem. A.* **110**, 1305 (2006).
- [34] C.-P. Hsu, S. Hirata, and M. Head-Gordon, *J. Phys. Chem. A* **105**, 451 (2001).
- [35] Z.-L. Cai, K. Sendt, and J. R. Reimers, *J. Chem. Phys.* **117**, 5543 (2002).
- [36] A. Dreuw and M. Head-Gordon, *J. Am. Chem. Soc.* **126**, 4007 (2004).
- [37] D. J. Tozer, R. D. Amos, N. C. Handy, B. O. Roos, and L. Serrano-Andres, *Molec. Phys.* **97**, 859 (1999).
- [38] M. E. Casida, F. Guiterrez, J. Guan, F.-X. Gadea, D. Salahub, and J.-P. Daudey, *J. Chem. Phys.* **113**, 7062 (2000).
- [39] S. Grimme and M. Parac, *Chem. Phys. Chem.* **4**, 292 (2003).
- [40] M. Parac, and S. Grimme, *Chem. Phys.* **292**, 11 (2003).
- [41] A. Drew, J. L. Weisman, and M. Head-Gordon, *J. Chem. Phys.* **119**, 2943 (2003).
- [42] N. N. Matsuzawa, A. Ishitani, D. Dixon, and T. Uda, *J. Phys. Chem. A* **105**, 4953 (2001).
- [43] A. Bernhardsson, N. Forsberg, P.-A. Malmqvist, B. O. Roos, and L. Serrano-Andres, *J. Chem. Phys.* **112**, 2798 (2000).